Environ. Eng. Res. 2015; 20(2): 181-189
http://dx.doi.org/10.4491/eer.2014.070

pISSN 1226-1025
eISSN 2005-968X

Sequential adsorption - photocatalytic oxidation process for wastewater treatment using a composite material TiO_2/activated carbon

Caroline Andriantsiferana[1†], Elham Farouk Mohamed[2], Henri Delmas[1]

[1]*Laboratoire de Génie Chimique, UMR CNRS 5503, University of Toulouse, Toulouse, France*
[2]*Department of Air Pollution, National Research Center, Dokki-Cairo 12622, Egypt*

ABSTRACT

A composite material was tested to eliminate phenol in aqueous solution combining adsorption on activated carbon and photocatalysis with TiO_2 in two different ways. A first implementation involved a sequential process with a loop reactor. The aim was to reuse this material as adsorbent several times with *in situ* photocatalytic regeneration. This process alternated a step of adsorption in the dark and a step of photocatalytic oxidation under UV irradiation with or without H_2O_2. Without H_2O_2, the composite material was poorly regenerated due to the accumulation of phenol and intermediates in the solution and on TiO_2 particles. In presence of H_2O_2, the regeneration of the composite material was clearly enhanced. After five consecutive adsorption runs, the amount of eliminated phenol was twice the maximum adsorption capacity. The phenol degradation could be described by a pseudo first-order kinetic model where constants were much higher with H_2O_2 (about tenfold) due to additional •OH radicals. The second implementation was in a continuous process as with a fixed bed reactor where adsorption and photocatalysis occurred simultaneously. The results were promising as a steady state was reached indicating stabilized behavior for both adsorption and photocatalysis.

Keywords: Activated carbon, Adsorption, Advanced oxidation process, Hydrogen peroxide, Photocatalysis, Titanium dioxide

1. Introduction

Advanced oxidation processes (AOPs) are widely used in wastewater treatment for the removal of organic and inorganic contaminants or to improve biodegradability of industrial wastewater. Heterogeneous photocatalytic process using TiO_2 as catalyst is one of the most promising AOPs. The radicals generated (OH•, O_2^{-}•, HOO•) can non-selectively mineralize a large range of organic pollutants which are difficult to eliminate [1]: pharmaceutical compounds [2, 3], dyes [4], pesticides [5], phenols [6], etc. Titanium dioxide (TiO_2) photocatalyst was broadly used because of its photochemical stability and comparatively low cost [7, 8, 9, 10]. However, the main drawback of the practical use of the TiO_2 is the difficulty to separate the TiO_2 powder from water. The need of an uneasy and costly final filtration limits the industrial-scale development of these photocatalytic processes. Therefore, to solve this problem, techniques have been developed for immobilizing TiO_2 catalyst onto the surface of a solid: sol-gel method [11], hydrothermal method [12], impregnation [13], atomic layer deposition [14], dip coating [15], hydrolysis [16], metal organic chemical vapour deposition [17, 18, 19], carbonization method [20], microwave irradiation [21]. The supporting materials generally suggested for degradation of organic compounds in water are materials such as silica, alumina, zeolites or clays [22], glass, quartz or steel [23, 24], activated carbon [17, 25] or membrane [26]. Improvement of photo-efficiency has not been systematically observed. Among these particle supports, activated carbon (AC) is very promising. Activated carbon adsorbs the pollutants and then releases them onto the surface of TiO_2. Consequently, the pollutants are more concentrated around the TiO_2 than in the bulk solution leading to an increase in the degradation rate of the pollutants [27, 28]. The intermediates produced during degradation could also be adsorbed onto activated carbon and then be oxidized. Other authors [29, 30, 31] have reported a synergistic effect for simple mixtures of AC and TiO_2, pollutants being more rapidly photodegraded in the mixed system which contains activated carbon. This so-called synergetic effect has been explained by the formation of a common contact interface between the different solid phases, in which AC acts as an efficient adsorption trap to the organic compounds. The pollutant is then more

Received October 15, 2014 **Accepted** May 19, 2015

† Corresponding author
Email: caroline.andriantsiferana@iut-tlse3.fr
Tel: +33-5-34-32-36-00 Fax: +33-5-34-32-36-97

efficiently transferred to the TiO_2 surface [32, 33, 34].

The main fundamental problem in using TiO_2 as photocatalyst is the energy loss in the electron-hole recombination which results in a lower efficiency of the degradation. Hence the prevention of electron-hole recombination becomes very important, the addition of electron acceptors into the reaction media is recommended: molecular oxygen present in air [35, 36] or H_2O_2 have been employed as effective electron acceptor in most photocatalysis applications. H_2O_2 could serve as electron scavenger to prevent the recombination and, in addition, generate more hydroxyl radicals [2]. In most of cases, the presence of H_2O_2 improved the photocatalytic oxidation performances [2, 27, 37] some authors reported a negative effect of H_2O_2 [38, 39, 40, 41]. Ilisz et al. [42] mainly observed the formation of primary oxidation products (hydroquinone, catechol and presumed aliphatics) at low concentration of H_2O_2 (< 0.01 mol/L) while hydroquinone and catechol concentration strongly decreased and ring-opening products were predominant at high H_2O_2 concentration (> 0.05 mol/L), more interesting in a complete degradation objective. Adan et al. [43] proposed the optimal molar ratio between concentrations of hydrogen peroxide and pollutant to be between 10 and 100.

In this work, phenol has been chosen as a model molecule representing hazardous phenol compounds in the industry. Indeed, phenolic compounds are identified as highly toxic compounds and non-biodegradable molecules. To degrade these compounds, a photocatalytic process has been implemented using commercial composite multilayer material TiO_2/AC. The photocatalytic activity of this material was evaluated in two different reactors and two different reaction modes. First, a sequential method of water treatment was carried out involving adsorption then photocatalytic oxidation in a loop reactor, with or without H_2O_2 to examine the improvement of photocatalysis by H_2O_2 addition. In this configuration, the water treatment was not achieved by oxidation but by adsorption, the oxidative step being needed only for pollutant degradation and *in situ* activated carbon regeneration. Then, the performance of the composite material was studied in a continuous annular reactor with simultaneous adsorption and photocatalysis.

2. Materials and Methods

2.1. Materials

Phenol (Bioxtra 99.5%) and hydrogene peroxide (30% w/w) were supplied by Sigma Aldrich.

Ahlstrom directly supplied the composite material TiO_2/AC, and separately the TiO_2 catalyst (PC 500, Millenium, anatase > 99%) and the AC. The composite material was a tissue composed with a mixture of synthetic fibers, acrylic polymer and granular activated carbon, a mixture of TiO_2 is coated on one side (EP1069950B1 European patent). The weight composition of this tissue is 4.5% TiO_2, 63.5% AC, 27.5% fibers, 4.5% SiO_2. SiO_2 was used as an inorganic binder for titanium deposited on the paper fibers. It is transparent with UV light and photo-stable. The granular activated carbon made from coconut with particle diameter in the range 250-600 μm, and its specific surface was 1,065 m^2/g. This activated carbon was mainly microporous (microporous and mesoporous volumes of 0.46 and 0.046 cm^3/g respectively). The diameter of the TiO_2 crystals was between 5 and 10 nm and the specific surface area S_{BET} about 320 m^2/g.

2.2. Analytical Methods

2.2.1. Solid analysis

The textural characterization was deduced from nitrogen adsorption at 77 K (ASAP 2010M; Micromeritics, Norcross, GA, USA). The specific surface area S_{BET} was determined from the BET method for relative pressure range (p/p_0) of 0.01-0.20 [44]. Methods from Horvath and Kawazoe [43] and Barrett et al. [44], referred as HK and BJH, were employed to assess the micropore and mesopore volumes respectively.

2.2.2. Liquid analysis

Phenol concentration measurements were performed by a high performance liquid chromatography equipment with UV detection at 254 nm (UV2000 dual wavelength; Thermo Finnigan, Les Ullis, France) using a C18 column (Prontosil, 4 mm × 250 mm i.d., 5 μm particles, I.C.S., Lapeyrouse-Fossat, France), with a mobile phase composed of acidified deionized water (W) (water acidified by H_3PO_4; pH = 2.2) and Acetonitrile (A) fed at 1 mL/min. The detector wavelength was set to 254 nm and the temperature of the column maintained at 30°C. For the adsorption step, an isocratic method was utilised (volumic composition Aqueous/Organic is 60/40). For the oxidation step, the separation of phenol from the oxidation intermediates was achieved with a mobile phase of variable volume composition W/A programmed at 1 mL/min (0-3 min: W only; 3-16 min: gradient W/A from 100/0 to 60/40; 16-25 min: 60/40).

The chemical oxygen demand (COD) was measured using colorimetric or digestion method with Hach equipment: a digital reactor block (DRB 200 HACH LANGE; Thermo Fisher Scientific, Illkirch, France), a spectrophotometer (DR/2500 HACH LANGE; Thermo Fisher Scientific, Illkirch, France) using 0-1,500 mg_{O2}/L range Hach tubes (potassium dichromate, salt of silver and mercury, sulfuric acid). The precision of the method was assessed with standard solutions and showed a standard deviation of less than 5%.

The total organic carbon (TOC) was also measured during photocatalytic oxidation step. First, the inorganic carbon present in the solution was eliminated with concentrated phosphoric acid (84%) and the solution was degassed by a current of nitrogen. The sample was then injected in a TOC-meter (TC Multi Analyser 2100 N/C; Analytic Jena, France) where the organic molecules were totally oxidized at 850°C, over a platinum catalyst. The quantity of CO_2 released by the reaction was then measured by infrared spectrometry (IR). Total organic carbon analysis was made when H_2O_2 was added in the oxidation step. Indeed, COD is no longer possible due to H_2O_2 interference in the dichromate method.

2.3. Experimental Set-ups and Procedures

2.3.1. Batch adsorption

Isotherms of the original granular AC and TiO_2/AC material were performed. In brown flasks, 0.5 g of adsorbent (AC or TiO_2/AC) was added to 100 mL of phenol solutions (0.5-5.0 g/L concentration range). The suspensions were left under stirring in a thermo-regu-

lated bath at 25°C for 8 days to ensure equilibrium. The solutions were not buffered, the final pH was in the range of 4 to 5. Then, the solutions were filtered on 0.25 μm nylon filter membranes before analysis [25]. The amount of adsorbed phenol was deduced from initial C_0 and final HPLC measurements of concentrations in the liquid phase.

2.3.2. The loop reactor

The 2 L batch loop reactor (Fig. 1) composed of a reactor section (0.65 L) and a recycling tank (1.35 L) was designed to operate with a sheet of composite TiO_2/AC (dimension: 360 mm × 120 mm × 3 mm; weight: 17 g with 10.9 g_{AC} and 0.8 g_{TiO_2}). The sheet was maintained barely immersed at the top of the flowing aqueous solution of phenol (C_0 = 0.88 g/L) which was circulated by a peristatic pump (MasterflexL/S; Thermo Fisher Scientific, Illkirch, France) at a constant flow rate (1,000 mL/min). The recycling tank was cooled by thermostatic water bath at 25°C (Julabo F12-ED; SELI, Toulouse, France). The equipment did not include the air supply as enough gas-liquid surface was available under both the composite sheet and the recycling tank to keep dissolved oxygen in the liquid. The range of emission of the 2 lamps (PL-L 24W; Philips, Bossee, France) was 340-400 nm with a maximum at 365 nm. The mean value of the light intensity measured with a radiometer (model RS232 Lutron; Thermo Fisher Scientific, Illkirch, France) was 55 W/m^2 at the surface of the composite material.

During the sequential process, two successive steps were achieved: adsorption then photo-oxidation corresponding to one cycle. The adsorption step was carried out in the dark during 4 days to approach the maximum loading corresponding to the adsorption equilibrium. Then, the oxidation step was started by switching on the UV lamps for 3 days. During the two steps samples were taken at regular time intervals and analysed by HPLC for determining the phenol concentration. A part of the samples was also used for measuring COD or TOC. TOC measurements have been chosen in presence of H_2O_2 in the oxidation step. After each oxidation step, the reactor was emptied from the oxidized solution of phenol and then filled by 2 L of a new one at same initial concentration (C_0 = 0.88 g/L) for starting a next cycle. High initial concentration of phenol has been chosen to quickly saturate the composite material and so show its regeneration.

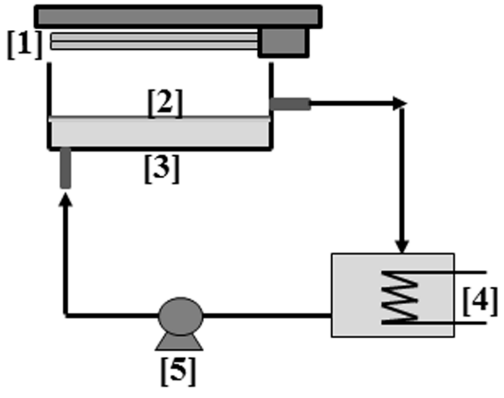

Fig. 1. Loop reactor; [1] 2 UV lamps, [2] Composite material TiO_2/AC, [3] loop reactor, [4] Intermediated thermo regulated reactor, [5] pump.

2.2.3. Annular continuous reactor

Experiments were carried out in an annular reactor of 120 mL shown in Fig. 2. On the central axis, the UV lamp was placed in a jacketed thermo-regulated cylinder (25°C). The mean value of the light intensity measured with the radiometer was 72 W/m (at the inside surface of the jacket cylinder). A peristaltic pump with a flow rate of 2 mL/min was used circulate the solution from the inlet tank to the annular reactor. The size of the sheet of composite TiO_2/AC was chosen to entirely fill the annular space ($m_{TiO2/AC}$ = 12.7 g, m_{TiO2} = 0.6 g). The experimental protocol was as follows. The composite material TiO_2/AC was pre-loaded in a beaker for 3 days using a solution of phenol (C_0 = 0.209 g/L) until the equilibrium was reached (C_{final} = 0.018 g/L). After this dark adsorption period, the oxidation process was then started using this loaded composite material as a pseudo-fixed bed in the annular reactor. As soon as the lamp was switched on, this reactor was continuously fed with a phenol solution, C_{inlet} = 0.018 g/L. The samples were taken each hour at the exit of the reactor via a sampling port. The experiment was conducted at 25°C. All samples were analysed by HPLC to determine the phenol concentrations.

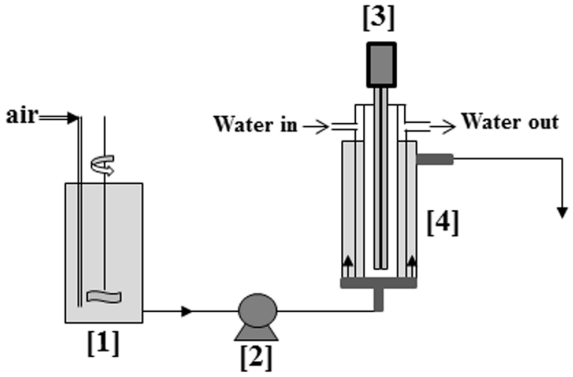

Fig. 2. Continuous reactor [1] aerated and stirred reactor, [2] pump, [3] UV lamp, [4] annular reactor.

3. Results and Discussion

3.1. Adsorption Isotherms

The adsorption isotherms of the original granular AC and TiO_2/AC material are presented in Fig. 3. Both isotherms exhibited the same shape, corresponding to type I of international union of pure applied chemistry classification (1985) as expected regarding the high AC microporosity (monolayer adsorption). Calculation of isotherm parameters has been performed using linearization of the Langmuir model equation. The Langmuir parameters given in Table 1 showed a higher value of the maximum adsorption capacity q_{max} (0.45 g/g) for the activated carbon alone. This saturation capacity was more important than the reported values in the literature for phenol adsorption. Usual values of q_{max} are between 0.20 and 0.35 g/g_{AC} under ambient temperature and unbuffered conditions showing the excellent performances of this activated carbon [47, 48, 49, 50, 51].

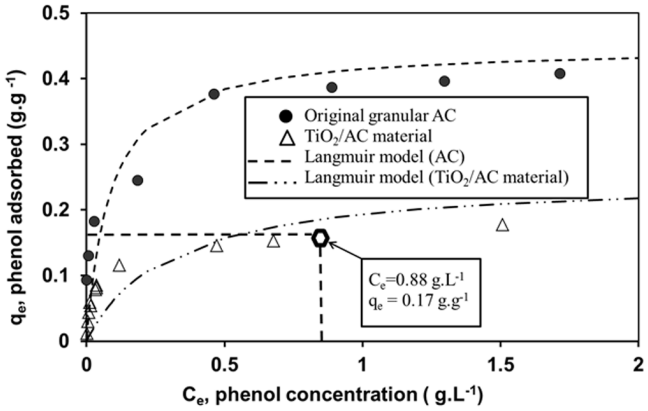

Fig. 3. Adsorption isotherms (Experimental and Langmuir model).

Table 1. Parameter Constants of Langmuir Model

Adsorbent	Parameters of Langmuir model $[q_e = q_{max}(C_eK_L)/(1+C_eK_L)]$		
	q_{max} (g/g)	K_L (L/g)	R^2
Granular AC	0.45	11.66	0.99
TiO_2/AC material	0.25	3.39	0.98

The composite material adsorption capacity is of course lower -as AC corresponds to only 63.5% of this material weight- but still very convenient. Note that in addition, when incorporated in the tissue, AC seems to lose about 12% of its specific adsorption capacity which could be due to partial pore clogging.

3.2. Sequential Process in Loop Reactor

3.2.1. Sequential process – 5 cycles without H_2O_2

Preliminary experiment with phenol and UV light was performed. Direct photolysis of phenol during 3,500 min did not change the concentration as expected from the absorbance spectrum of phenol (no absorbance above 310 nm). Five cycles of adsorption-photocatalytic regeneration have been carried out with the composite material (Fig. 4(a) and (b)). In comparison with classic adsorption kinetics with granular carbon, the kinetics were very slow probably due to the diffusion limitation of the phenol inside the layer of natural and synthetic fibers containing AC. Table 2 showed a gradually decrease of the quantities adsorbed and the regeneration efficiency R_e calculated from Eq. (1).

$$R_e = \frac{\text{Quantity adsorbed (cycle i)}}{\text{Quantity adsorbed (cycle 1)}} \quad \text{where} \quad i = 1 \text{ to } 5 \quad (1)$$

The total quantity of adsorbed phenol (0.218 g/g) was 40% higher than the theoretical maximum adsorbed amount for a concentration equal to 0.88 g/L (0.17 g/g, see isotherm on Fig. 3) proving the effective regeneration of the composite material. The final degraded fraction decreased from 95% at cycle 1 to 1% at cycle 5 due to an incomplete regeneration of the material. The first-order kinetic model (Eq. (2)) was used to describe the kinetics of phenol degradation (Fig. 4(b)) and to obtain the values of the apparent constant of degradation at each cycle.

$$r = -\frac{dc}{dt} = k_{app}c \quad (2)$$

The model fitted well until about one hour, then the presence of an important quantity of intermediates (hydroquinone, catechol, benzoquinone, aliphatic compounds, etc.) and the competitive adsorption between phenol and these intermediates might change kinetics [52]. Consequently, the calculation of k_{app} was done using the first part of these kinetics. Decrease of the successive apparent contants k_{app} confirmed the continuous degradation of the regeneration efficiency and the pseudo-first order of the kinetic (depending on total concentration). This phenomenon was classically observed in photocatalysis when high quantity of organic molecules had to be degraded [53]. Above a certain level of phenol concentration, the catalyst surface becomes saturated, and this may even lead to a decrease in the observed rates [54]. The COD evolution was represented in Fig. 5. The degradation did not exceed 5% for the 4th cycle. For the first cycle, even if 95% of the phenol was removed in the liquid phase, 40% of the initial COD remained in solution due to the reaction intermediates. At the end of each oxidation step, the contribution of phenol to the COD was calculated using phenol concentration (HPLC): 15%, 42%, 80% and 84% for the 1st, 2nd, 3rd and 4th cycles respectively (Table 2). These results confirmed that the conditions of oxidation were degraded from the second cycle.

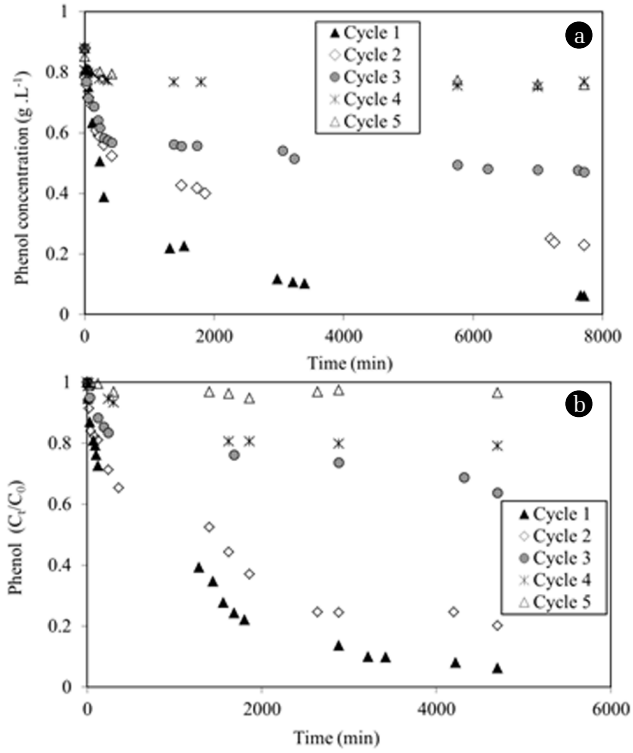

Fig. 4. Evolution of the phenol concentration - Sequential process without H_2O_2; (a) Adsorptions, C_0 = 0.88 g/L; (b) Oxidations under UV irradiation, $[TiO_2]$ = 0.4 g/L.

Table 2. Sequential Process with the Loop Reactor. Influence of the Presence of H_2O_2 on Comparative Parameters

	Cycle	1	2	3	4	5	Total
Without H_2O_2	Adsorbed quantity (g/g)	0.093	0.074	0.024	0.013	0.014	0.218
	Regeneration efficiency R_e[a] (%)	100	80	26	13	14	-
	Initial phenol concentration[b] (g/L)	0.062	0.228	0.469	0.768	-	-
	First order apparent constant K_{app}[c] (min^{-1})	0.0046	0.0042	0.0017	0.0017	-	-
	Final degradated fraction[d] (%)	95	80	37	20	1	-
	Initial COD[e] (mg/L)	150	545	1,120	1,830	-	-
	Final COD[f] (mg/L)	60	260	900	1,721	-	
	Final COD_{phenol}[g] (%)	9	110	713	1,448	-	-
With H_2O_2	Adsorbed quantity (g/g)	0.0945	0.0903	0.0827	0.0630	0.059	0.389
	Regeneration efficiency R_e[a] (%)	100	95	87	66	62	-
	Initial phenol concentration[b] (g/L)	0.054	0.093	0.159	0.332	0.365	-
	First order apparent constant K_{app}[c] (min^{-1})	0.057	0.017	0.011	0.010	0.008	-
	Final degradated fraction[d] (%)	100	100	97	97	96	-
	Initial TOC[e] (mg/L)	54	345	475	443	627	-
	Final TOC[f] (mg/L)	17	152	240	161	177	
	Final TOC_{phenol}[h] (mg/L)	0	0	0	7	9	

a: regeneration efficiency calculated with Eq. (1)
b: phenol concentration at the beginning of each oxidation step
c: first-order apparent constant Kapp: $\ln\frac{c}{c_0} = -K_{app}\,t$ from Eq. (2)
d: final degradated fraction $= \frac{\text{Quantity phenol eliminated}}{\text{Quantity phenol initial}} \times 100$
e: initial COD or TOC: COD or TOC at the beginning of each oxidation step
f: final COD or TOC: COD or TOC at the end of each oxidation step
g: Calculated from HPLC phenol molar concentration ($C_6H_6O+7O_2 \rightarrow 6CO_2 + 3H_2O$);
h: Calculated from HPLC phenol molar concentration (TOC = 6 × 12 × [phenol]).

At the end of the 5th cycle, the activated carbon inside the composite material was analyzed. The surface area S_{BET} was reduced by 80% (from 1,065 m^2/g to 208 m^2/g) and the microporous volume by 84% (from 0.460 cm^3/g to 0.076 cm^3/g). An important quantity of phenol and oxidation intermediates were accumulated in the micropores without being further oxidized. These molecules deeply adsorbed in these pores did not migrate from the activated carbon to the catalyst to be degraded. The expected mechanism (adsorption of phenol → phenol diffusion from AC to TiO_2 → total phenol mineralization under UV → total regeneration of the composite material) was no longer taking place. At the photo-catalyst surface, the phenol and intermediates remained concentrated and cycle after cycle more organic compounds get adsorbed. The photocatalytic activity decreased due to the accumulation of reaction intermediates formed at the surface as a result of partial oxidation of phenol. The presence of these molecules reduced number of reaction sites and reactivity with time. The catalyst used presented a low selectivity toward total oxidation with respect to partial oxidations [14]. This loss of activity might suggest a poisoning of the surface of the catalyst. Another explanation could be proposed: at the surface of the catalyst, these intermediates were probably in competition with H_2O and O_2 on the adsorption sites. Then less molecules of water and oxygen would be adsorbed at the surface of the catalyst, therefore, an increase of the recombination of the electron/hole pairs could occur. This phenomenon could explain a lower production of oxidative species ($OH^{\bullet}$ and $O_2^{-\bullet}$) and an additional loss of photo-activity.

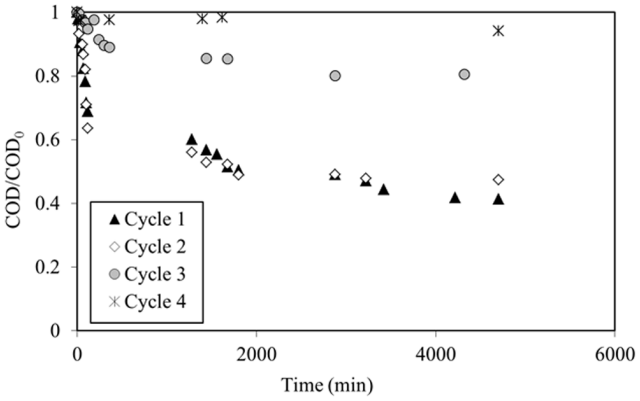

Fig. 5. Carbon oxygen demand (COD) removal during 4 cycles, [TiO_2] = 0.4 g/L.

3.2.2. Sequential process – 5 cycles with H_2O_2

In order to improve the oxidation process the effect of H_2O_2 addition on the rate of phenol degradation was investigated. At the beginning of each oxidation step, 50 mL of H_2O_2 (30% weight) were added to the solution. For the first oxidation, the corresponding initial H_2O_2/phenol molar ratio = 24 was almost twice the stoichiometric amount of hydrogen peroxide for complete mineralization, in agreement with the values proposed by Adan et al. [43] in the range 10 to 100). In presence of H_2O_2, Fig. 6(a) showed an effective

adsorption for all of the five cycles. The amount of adsorbed phenol decreased, but much more slowly than without H_2O_2 and the regeneration efficiency remained superior to 60%: the regeneration was still partly achieved even after 5 cycles (Table 2). The total quantity of phenol adsorbed during 5 cycles (0.389 g/g) was 140% superior to the theoretical maximum amount adsorbed (see Fig. 3) and almost twice the quantity eliminates without H_2O_2. From these results, the coupling of H_2O_2 and TiO_2 significantly improved the performance of the AC regeneration. As shown in Fig. 6(b), the phenol degradation was only slightly decreased from 100% to 96%. The pseudo first-order kinetic model (Eq. (2)) fitted well, the apparent constant k_{app} were between 4 and 12 times higher than without H_2O_2 (Table 2). The intermediates degradation has gone further as shown by the evolution of the TOC in Fig. 7. Indeed, the TOC conversion rate was between 60% and 70%. The comparison between total TOC and phenol contribution TOC phenol showed an important presence of intermediates (Table 2) showing the partial oxidation of the phenol. This is in agreement with Zhang et al. [55] who reported rather high values of TOC even at total degradation of the aromatic molecules. These intermediates product are thought to be aliphalic acids known to be difficult to oxidize [56].

For the first cycle, the synergetic factor S, calculated with Eq. (3), was equal to 7.5 confirming the better photocatalytic performance with H_2O_2.

$$S = \frac{k_{app,\ with\ H_2O_2}}{k_{app,\ without\ H_2O_2} + k_{app,\ alone}} \quad (3)$$

Where:

k_{app} (with H_2O_2) is the value of k_{app} with the composite material, with H_2O_2 and with UV

k_{app} (without H_2O_2) is the value of k_{app} with the composite material and with UV

k_{app} (alone) is the value of k_{app} without the composite material and with UV (reference).

This better performance was due to two additional pathways of •OH production in presence of H_2O_2 [41, 57]:

Pathway 1: $H_2O_2 + \text{electron} \rightarrow {\bullet}OH + OH^-$ (4)

Pathway 2: $O_2 + \text{electron} \rightarrow {\bullet}O_2^-$ (5)

$$H_2O_2 + {\bullet}O_2^- \rightarrow {\bullet}OH + OH^- + O_2 \quad (6)$$

The quantity of added H_2O_2 was chosen in agreement with literature to avoid the negative effect of H_2O_2. Indeed, introduced in excess, H_2O_2 could react with hydroxyl radicals and the holes (reactions (7) and (8)): a weaker oxidizing radical $\bullet HO_2$ being produced, inducing a decrease of the photocatalytic performances [2].

$$H_2O_2 + {\bullet}OH \rightarrow H_2O + {\bullet}HO_2 \quad (7)$$

$$H_2O_2 + \text{hole} \rightarrow H^+ + {\bullet}HO_2 \quad (8)$$

After the 5th cycle, the AC present in the composite material was analyzed and compared to the virgin one: the surface area S_{BET} was reduced by 47% (from 1,065 m^2/g to 562 m^2/g) and the microporous volume by 75% (from 0.460 cm^3/g to 0.113 cm^3/g). In comparison with experiments without H_2O_2, this better preservation of surface area and porous volume proved phenol and intermediates to be less accumulated in the pores leading to more efficient regeneration.

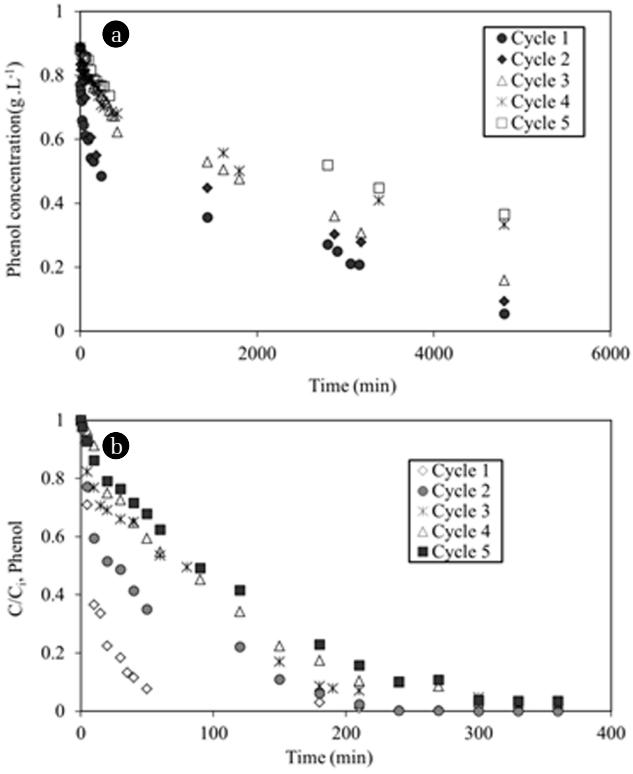

Fig. 6. Evolution of the phenol concentration - Sequential process during 5 cycles in presence of H_2O_2; (a) Adsorptions (C_0 = 0.88 g/L), (b) Oxidations under UV irradiation, [TiO_2] = 0.4 g/L, [H_2O_2] = 7.6 g/L.

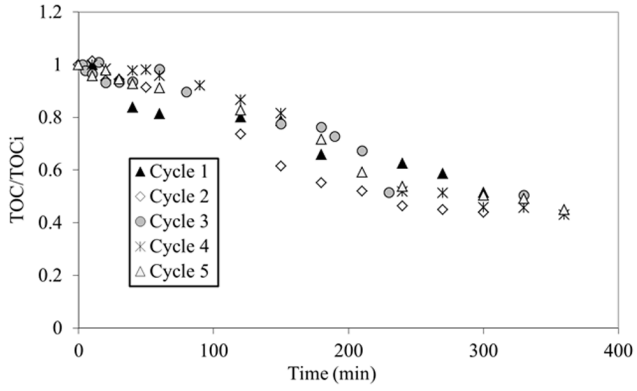

Fig. 7. Total organic carbon (TOC) removal with H_2O_2; [TiO_2] = 0.4 g/L, [H_2O_2] = 7.6 g/L.

3.3. Continuous Annular Reactor

In continuous mode, adsorption and photocatalytic oxidation operated simultaneously. Under UV light, Fig. 8 shows a transient

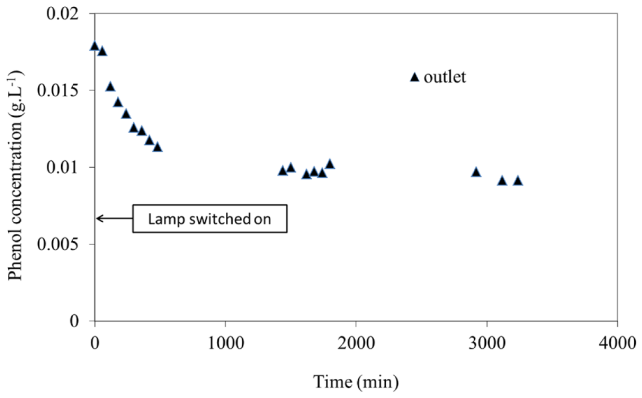

Fig. 8. Evolution of the phenol concentration using continuous reactor during UV irradiation; C_{inlet} = 0.017 g/L, m_{TiO_2} = 12.7 g.

behaviour with initial decreasing phenol concentration due to the added photocatalytic activity. Then the steady state was obtained corresponding to equilibrium between adsorption and oxidation and proving the composite to get a stable behaviour without noticeable deactivation. In these conditions, 55% of the phenol was removed corresponding to an overall reaction rate of 5 10^{-6} (g_{phenol}/g_{TiO_2}) s^{-1}.

4. Conclusions

This study was conducted to put on the map an innovative process to degrade aromatic molecules. To offer an economically interesting process, the conditions were: (1) to use a commercial material and cheap UV lamps; (2) to prolong the adsorption activity of the material with *in situ* regeneration.

A first implementation was involved using a loop reactor. This sequential process alternated 5 cycles with a step of adsorption in dark and a step of photocatalytic oxidation under UV irradiation. Without H_2O_2, the regeneration of the composite multilayer material became ineffective from the third cycle on. Cycle after cycle, more pollutants were present at the surface of the composite material and in the solution. The apparent constants decreased drastically, reaction intermediates accumulated on the surface of the photocatalyst, reducing number of reaction sites and reactivity with time. After several uses, this accumulation induced a poisoning of the catalyst. The presence of H_2O_2 improved the conditions of regeneration. For the 5 cycles, the phenol degradation was between 100% and 96% and the TOC conversion rate was between 60% and 70%. At industrial scale, the process could be implemented as follow: (1) a step of continuous adsorption by controlling the outlet concentration; (2) a step of regeneration in batch mode using a small volume of water and in presence of UV and H_2O_2 controlling and optimizing the quantity of UV light, the catalyst loading and the duration of irradiation.

Acknowledgements

The authors wish to acknowledge Cedric Vallet from Ahlstrom who supplied all material.

References

1. Lagunas-Allue L, Martinez-Soria MT, Sanz-Asensio J, Salvador A, Ferronato C, Chovelon JM. Photocatalytic degradation of boscalid in aqueous titanium dioxide suspension: Identification of intermediates and degradation pathways. *Appl. Catal.* B 2010;98:122-131.
2. Elmolla ES, Chaudhuri M. Photocatalytic degradation of amoxicillin, ampicillin and cloxacillin antibiotics in aqueous solution using UV/TiO_2 and UV/H_2O_2/TiO_2 photocatalysis. *Desalination* 2010;252:46-52.
3. HHH Lin, AYC Lin. Photocatalytic oxidation of 5-fluorouracil and cyclophosphamide via UV/TiO_2 in an aqueous environment. *Water Res.* 2014;48:559-568.
4. Konstantinou IK, Albanis TA. TiO_2-assisted photocatalytic degradation of azo dyes in aqueous solution: kinetic and mechanistic investigations. A review. *Appl. Catal. B* 2004;49:1-14.
5. Rizzo L. Bioassays as a tool for evaluating advanced oxidation processes in water and wastewater treatment. *Water Res.* 2011;45:4311-4340.
6. Benoit-Marquié F, Puech-Costes E, Braun A, Oliveros E, Maurette MT. Photocatalytic degradation of 2,4-dihydroxybenzoïc acid in water : efficiency optimization and mechanistic investigation. *J. Photochem. Photobiol. A chem.* 1997;108: 65-71.
7. Arana J, Melian JAH, Rodriguez JMD, et al. TiO_2-photocatalysis as a tertiary treatment of naturally treated wastewater. *Catal. Today* 2002;76:279-289.
8. Areerachakul N, Vigneswaran S, Ngo HH, Kandasamy J. Granular activated carbon (GAC) adsorption–photocatalysis hybrid system in the removal of herbicide from water. *Sep. Purif. Technol.* 2007;55:206-211.
9. Zhang L, Kanki T, Sano N, Toyoda A. Development of TiO_2 photocatalyst reaction for water purification. *Sep. Purif. Technol.* 2003;31:105-110.
10. Shon HK, Vigneswaran S, Ngo HH, Kim JH. Chemical coupling of photocatalysis with flocculation and adsorption in the removal of organic matter. *Water Res.* 2005;39:2549-2558.
11. Lee DK, Kim SC, Cho IC, Kim SJ, Kim SW. Photocatalytic oxidation of microcystin-LR in a fluidized bed reactor having TiO_2-coated activated carbon. *Sep. Purif. Technol.* 2004;34: 59-66.
12. Toyoda M, Nanbu Y, Kito T, Hiranob M, Inagaki M. Preparation and performance of anatase-loaded porous carbons for water purification. *Desalination* 2003;159:273-282.
13. Tao Y, Schwartz S, Wu CY, Mazyck DW. Development of a TiO_2/AC composite photocatalyst by dry impregnation for the treatment of methanol in humid airstreams. *Ind. Eng. Chem. Res.* 2005;44:7366-7372.
14. Kim KD, Dey NK, Seo HO, Kim YD, Lim DC, Lee M. Photocatalytic decomposition of toluene by nano-diamond supported TiO_2 prepared using atomic layer deposition. *Appl. Catal. A: Gen.* 2011;408:148-155.
15. Sun J, Wang X, Sun J, Sun R, Sun S, Qiao L. Photocatalytic degradation and kinetics of Orange G using nano-sized Sn(IV)/TiO_2/AC photocatalyst. *J. Mol. Catal. A Chem.* 2006;

260:241-246.
16. El-Sheikh AH, Newman AP, Al-Daffaee H, Phull S, Cresswell N, York S. Deposition of anatase on the surface of activated carbon. *Surf. Coat. Technol.* 2004;187:284-292.
17. Andriantsiferana C, Mohamed EF, Delmas H. Photocatalytic degradation of an azo-dye on TiO_2/activated carbon composite material. *Environ. Technol.* 2014;35:355-363.
18. Mills A, Elliott N, Parkin IP, O'Neill SA, Clark RJ. Novel TiO_2 CVD films for semiconductor photocatalysis. *J. Photochem. Photobiol. A Chem.* 2002;151:171-179.
19. Zhang X, Zhou M, Lei L. Preparation of photocatalytic TiO_2 coatings of nanosized particles on activated carbon by AP-MOCVD. *Carbon* 2005;43:1700-1708.
20. Teng F, Zhang G, Wang Y, et al. The role of carbon in the photocatalytic reaction of carbon/TiO_2 photocatalysts. *Appl. Surf. Sci.* 2014;320:703-709.
21. Horikoshi S, Sakamoto S, Serpone N. Formation and efficacy of TiO_2/AC composites prepared under microwave irradiation in the photoinduced transformation of the 2-propanol VOC pollutant in air. *Appl. Catal. B* 2013;140-141:646-651.
22. Tanguay JF, Suib SL, Coughlin RW. Dichloromethane photodegradation using titanium catalysts. *J. Catal.* 1989;117: 335-347.
23. Fernandez A, Lassaletta G, Jimenez VM, et al. Preparation and characterization of TiO_2 photocatalysts supported on various rigid supports (glass, quartz and stainless steel), Comparative studies of photocatalytic activity in water purification. *Appl. Catal. B* 1995;7:49-63.
24. Zazueta ALL, Destaillats H, Puma GL. Radiation field modeling and optimization of a compact and modular multi-plate photocatalytic reactor (MPPR) for air/water purification by Monte Carlo method. *Chem. Eng. J.* 2013;217:475-485.
25. Matos J, Laine J, Hermann JM. Effect of the type of activated carbons on the photocatalytic degradation of aqueous organic pollutants by UV-irradiated titania. *J. Catal.* 2001;200:10-20.
26. Goei R, Lim TT. Asymmetric TiO_2 hybrid photocatalytic ceramic membrane with porosity gradient: Effect of structure directing agent on the resulting membranes architecture and performances. *Ceram. Int.* 2014;40:6747-6757.
27. Tryba B, Morawski AW, Inagaki M. Application of TiO_2- mounted activated carbon to the removal of phenol from water. *Appl. Catal. B* 2003;41:427-433.
28. Tsumura T, Kojitani N, Umemura H, Toyoda M, Inagaki M. Composites between photoactive anatase-type TiO_2 and adsorptive carbon. *Appl. Surf. Sci.* 2002;196:429-436.
29. Herrmann JM. Heterogeneous photocatalysis: fundamentals and applications to the removal of various types of aqueous pollutants. *Catal. Today* 1999;53:115-129.
30. Matos J, Laine J, Hermann JM, Uzcategui D, Brito JL. Influence of activated carbon upon titania on aqueous photocatalytic consecutive runs of phenol photodegradation. *Appl. Catal. B* 2007;70:461-469.
31. García-Munoz P, Carbajo J, Faraldos M, Bahamonde A. Photocatalytic degradation of phenol and isoproturon: Effect of adding an activated carbon to titania catalyst. *J. Photochem. Photobiol. A Chem.* 2014;287:8-18.
32. Ao CH, Lee SC. Enhancement effect of TiO_2 immobilized on activated carbon fiber for the photodegradation of pollutants at typical indoor air level. *Appl. Catal. B* 2003;44:191-205.
33. Chiang YC, Chiang PC, Huang CP. Effects of pore structure and temperature on VOC adsorption on activated carbon. *Carbon* 2001;39:523-534.
34. Wang JP, Chen YZ, Feng HM, Zhang SJ, Yu HQ. Removal of 2,4 - dichlorophenol from aqueous solution by static-air-activated carbon fibers. *J. Colloid Interface Sci.* 2007;313: 80-85.
35. Augugliaro V, Palmisano L, Schiavello M, Sclafani A. Photocatalytic degradation of nitrophenols in aqueous titanium dioxide dispersion. *Appl. Catal.* 1991;69:323-340.
36. Gupta H, Tanaka S. Photocatalytic mineralisation of perchlororthylene using titanium dioxide. *Water Sci. Technol.* 1995;31:47-54.
37. Herrmann JM, Guillard C, Pichat P. Heterogeneous photocatalysis: an emerging technology for water treatment. *Catal. Today* 1993;17:7-20.
38. Chu W. Modeling the quantum yields of herbicide 2,4-D decay in UV/H_2O_2 process. *Chemosphere* 2001;44:935-941.
39. Dionysiou DD, Suidan MT, Baudin I, Laine JM. Effect of hydrogen peroxide on the destruction of organic contaminants-synergism and inhibition in a continuous-mode photocatalytic reactor. *Appl. Catal. B* 2004;50:259-269.
40. Chen S, Liu Y. Study on the photocatalytic degradation of glyphosate by TiO_2 photocatalyst. *Chemosphere* 2007;67: 1010-1017.
41. Achilleos A, Hapeshi E, Xekoukoulotakis NP, Mantzavinos D, Fatta-Kassinosa D. Factors affecting diclofenac decomposition in water by UV-A/TiO_2 photocatalysis. *Chem. Eng. J.* 2010;161:53-59.
42. Ilisz I, Laszlo Z, Dombi A. Investigation of the photodecomposition of phenol in near-UV-irradiated aqueous TiO_2 suspension. I: Effect of charge-trapping species on the degradation kinetic. *Appl. Catal. A* 1999;180:25-33.
43. Adan C, Carbajo J, Bahamonde A, Martinez-Arias A. Phenol photodegradation with oxygen and hydrogen peroxide over TiO_2 and Fe-doped TiO_2. *Catal. Today* 2009;143:247-252.
44. Brunauer S, Emmett PH, Teller E. Adsorption of gases in multimolecular layers. *J. Am. Chem. Soc.* 1938;60:309-319.
45. Horvath G, Kawazoe KJ. Method for the calculation of effective pore size distribution in molecular sieve carbon. *J. Chem. Eng. Japan* 1983;16:470-475.
46. Barrett EP, Joyner LG, Halenda PP. The determination of pore volume and area distributions in porous substances. *J. Am. Chem. Soc.* 1951;73:373-380.
47. Laszlo K, Tombacz E, Novak C. pH-dependent adsorption and desorption of phenol and aniline on basic activated carbon. *Colloids Surf. A Physicochem. Eng. Asp.* 2007;306:95-101.
48. Kumar A, Kumar S, Kumar S, Gupta DV. Adsorption of phenol and 4-nitrophenol on granular activated carbon in basal salt medium: Equilibrium and kinetics. *J. Hazard. Mater.* 2007;147:155-166.
49. Liu C, Tang Z, Chen Y, Su S, Jiang W. Characterization of mesoporous activated carbons prepared by pyrolysis of sewage

sludge with pyrolusite. *Bioresour. Technol.* 2010;101:1097-1101.
50. Andriantsiferana C, Julcour-Lebigue C, Creanga-Manole C, Delmas H, Wilhelm AM. Competitive Adsorption of p-Hydroxybenzoic Acid and Phenol on Activated Carbon: Experimental Study and Modeling. *J. Environ. Eng.* 2013;139: 402-409.
51. Mohamed EF, Andriantsiferana C, Wilhelm AM, Delmas H. Competitive adsorption of phenolic compounds from aqueous solution using sludge based activated carbon. *Environ. Technol.* 2011;32:1325-1336.
52. Cordero T, Duchamp C, Chovelon JM, Ferronato C, Matos J. Influence of L-type activated carbons on photocatalytic activity of TiO_2 in 4-chlorophenol photodegradation. *J. Photochem. Photobiol. A Chem.* 2007;191:122-131.
53. Ahmed S, Rasul MG, Martens WN, Brown R, Hashib MA. Heterogeneous photocatalytic degradation of phenols in wastewater: a review on current status and developments. *Desalination* 2010;261:3-18.
54. Grabowska E, Reszczynska J, Zaleska A. Mechanism of phenol photodegradation in the presence of pure and modified-TiO_2: A review. *Water Res.* 2012;46:5453-5471.
55. Zhang X, Li A, Jiang Z, Zhang Q. Adsorption of dyes and phenol from water on resin adsorbents: effect of adsorbate size and pore size distribution. *J. Hazard. Mater.* 2006;137: 1115-1122.
56. Santos A, Yustos P, Quintanilla A, Rodriguez S, Garcia-Ochoa F. Route of the catalytic oxidation of phenol in aqueous phase. *Appl. Catal. B* 2002;39:97-113.
57. Muruganandham M, Swaminathan M. Photocatalytic decolourisation and degradation of Reactive Orange 4 by TiO_2-UV process. *Dyes Pigm.* 2006;68:133-142.